Supramolecular Assembly of Mg(II) Complexes Directed by Associative Lone Pair−π/π−π/π−Anion−π/π−Lone Pair Interactions

Amrita Das,[†] Somnath Ray Choudhury,*[,†] Biswajit Dey,[‡] Sampath Kumar Yalamanchili,[§] Madeleine Helliwell,[§] Patrick Gamez,[||] Subrata Mukhopadhyay,*[,†] Carolina Estarellas,[⊥] and Antonio Frontera[⊥]

Department of Chemistry, Jadavpur University, Kolkata 700 032, India, Department of Chemistry, Visva-Bharati, Santiniketan 731 235, West Bengal, India, School of Chemistry, The University of Manchester, Brunswick Street, Manchester, M13 9PL, U.K., Leiden Institute of Chemistry, Leiden University, P.O. Box 9502, 2300 RA Leiden, The Netherlands, and Department of Chemistry, Universitat de les Illes Balears, Crta. de Valldemossa km 7.5, 07122 Palma de Mallorca (Baleares), Spain

Received: December 16, 2009; Revised Manuscript Received: March 16, 2010

Two Mg(II) malonate complexes with protonated 2-aminopyridine and protonated 2-amino-4-picoline as counterions, namely, $(C_5H_7N_2)_4[Mg(C_3H_2O_4)_2(H_2O)_2](ClO_4)_2$ (**1**) and $(C_6H_8N_2H)_2[Mg(C_3H_2O_4)_2(H_2O)_2]\cdot 4H_2O$ (**2**) [$C_5H_7N_2$ = protonated 2-aminopyridine, $C_3H_4O_4$ = malonic acid, $C_6H_8N_2H$ = protonated 2-amino-4-picoline], have been synthesized from purely aqueous media, and their crystal structures have been determined by single-crystal X-ray diffraction. The role of lone pair$\cdots\pi$ interactions in stabilizing the self-assembly process appears to be of great importance in both complexes. Additional weak forces like anion$\cdots\pi$ and noncovalent O$\cdots$O interactions are also found to be operating in **1**. A rare combination of lone pair$\cdots\pi$ and anion$\cdots\pi$ interactions in **1**, of the type lone pair$\cdots\pi/\pi\cdots\pi/\pi\cdots$anion$\cdots\pi/\pi\cdots$lone pair, is observed, and this unusual supramolecular network is fully described here. An attempt to prepare an analogous complex with 2-amino-4-picoline resulted in **2**, which is isomorphous with our recently reported transition-metal complexes of the type $(C_6H_8N_2H)_2[M(C_3H_2O_4)_2(H_2O)_2]\cdot 4H_2O$ (M = Ni/Co/Mn). A high-level DFT-D study (RI-B97-D/TZVP) has been used to characterize the different noncovalent interactions present in the solid state. We have also analyzed some crystal fragments to examine energetically some important assemblies that drive the crystal packing. Finally, we have studied the influence of magnesium on some hydrogen-bonding interactions.

Introduction

The field of crystal engineering is rapidly expanding as a global discipline practiced by scientists with diverse interests, without traditional boundaries. It deals with modeling, synthesis, evaluation, and utilization of crystalline solids having desired functions, as well as fascinating topological architectures.[1–10] However, the full potential of this multidisciplinary branch of science is yet to be realized. The principle of designed synthesis of functional materials has to some extent been rationalized, but any successful crystal engineering experiment tends to be difficult to control, due to the delicate nature of a number of competing weak forces.[8,11] Therefore, crystal structure prediction is a formidable exercise and is very far from being fully resolved. The key to crystal structure prediction is a precise understanding and a complete control over the interplay of weak interactions responsible for crystal packing, when a number of them are operating simultaneously.[11–14]

Various weak dispersive interactions, such as hydrogen-bonding,[7,15–19] $\pi\cdots\pi$ stacking,[20–23] cation$\cdots\pi$,[24] and C−H$\cdots\pi$[25,26] contacts, are very common and well accepted among the supramolecular chemists. For around five years, a new type of supramolecular interaction, namely, the anion$\cdots\pi$,[27–29] has been increasingly reported in the literature, notwithstanding the preliminary improbability of considering repulsive interactions among the aromatic clouds and electron rich molecules in such instances.[30–35] Egli and co-workers have extended this concept to a more general form, namely, lone pair$\cdots\pi$ interactions.[36] They reported two clear cases of lone pair$\cdots\pi$ interactions in biomacromolecules: (a) the stabilization of the structure of *Z*-DNA[37,38] and (b) $H_2O\cdots\pi$ interactions within a ribosomal frame-shifting RNA pseudoknot.[39] Indeed, lone pair$\cdots\pi$ interactions have been found to be of great importance for the stabilization of biological macromolecules, as well as for the binding of inhibitors in the binding pocket of biochemical receptors.[40] Very recently, in a comprehensive review,[41] Gamez et al. designated such lone pair$\cdots\pi$ contacts as a new supramolecular bond and rigorous analysis of the Cambridge Structure Database (CSD) revealed that such contacts are not unusual in organic/coordination compounds but have been overlooked in the past. This thorough survey of the CSD clearly shows that lone pair$\cdots\pi$ interactions are actually ubiquitous in solid-state structures (such as the supramolecular anion$\cdots\pi$ contacts[32]). Surprisingly, only a few examples of lone pair$\cdots\pi$ interactions involving small synthetic molecules have been reported, rendering this topic as "hardly studied".[42] Therefore, current research investigations are aimed at systematically studying this type of noncovalent bonding interactions observed in new crystal structures, to gain knowledge in this nascent field, both theoretically and experimentally. In that context, our serendipi-

* To whom correspondence should be addressed. E-mail: som_rc_ju@yahoo.co.in (S.R.C.); smukhopadhyay@chemistry.jdvu.ac.in (S.M.).
[†] Jadavpur University.
[‡] Visva-Bharati.
[§] The University of Manchester.
[||] Leiden University.
[⊥] Universitat de les Illes Balears.

10.1021/jp911884x
Published on Web 03/31/2010

tous discovery of carbonyl(lone pair)···π/π···π/carbonyl(lone pair)···π and carbonyl(lone pair)···π/π···π/π···anion supramolecular associations in the solid-state structure of some transition-metal− and non-transition-metal−organic hybrid complexes sheds light on the potentiality of such newly discovered supramolecular forces in organizing and stabilizing molecular components in crystals.[43,44]

Besides noncovalent interactions[45,46] involving aromatic π systems, intensive structural investigations in the fields of biopolymers and organic conductors have shown that weak interactions between chalcogen centers contribute considerably to stabilize conformations.[47–49] van der Waals interactions between sulfur centers have been encountered in a number of cases, particularly in crystal engineering of organic conductors such as tetrathiafulvalene (TTF) and tetracyanoquinodimethane (TCNQ).[47,48] These studies revealed that close S···S contacts play an important role in the formation of two- and three-dimensional networks in the solid state. Recent reports also support the importance of S···S interaction in supramolecular architectures.[11,50–55] Noncovalent O···O interactions are also well-established in the literature, including their theoretical aspects.[56–63] Raghavaiah et al. found for the first time that short O···O contacts played a decisive role in the construction of a helix.[64] Some comprehensive theoretical investigations on model systems to understand the nature of intermolecular interactions between chalcogen centers are also available in the literature.[65–67] We also study herein the unusual role of perchlorate anions to construct a 2D assembly of $[Mg(C_3H_2O_4)_2(H_2O)_2]^{2-}$ anionic units in **1** through O···O short contacts.

In this report, the synthesis, structural determination, and routine physicochemical analyses of two Mg(II) malonate complexes, namely, $(C_5H_7N_2)_4[Mg(C_3H_2O_4)_2(H_2O)_2](ClO_4)_2$ (**1**) and $(C_6H_8N_2H)_2[Mg(C_3H_2O_4)_2(H_2O)_2]\cdot 4H_2O$ (**2**), are described. Complex **1** is related to our previously reported $(C_5H_7N_2)_4[Ni(C_3H_2O_4)_2(H_2O)_2](NO_3)_2$ and $(C_5H_7N_2)_4[Mg(C_3H_2O_4)_2(H_2O)_2](NO_3)_2$ coordination compounds,[43,44] whereas complex **2** is isomorphous with our recently communicated related transition-metal complexes $(C_6H_8N_2H)_2[M(C_3H_2O_4)_2(H_2O)_2]\cdot 4H_2O$ ($C_6H_8N_2H$ = protonated 2-amino-4-picoline, M = Ni/Co/Mn, $C_3H_4O_4$ = malonate).[68] The self-assembly of the two complexes is analyzed, and an outstanding supramolecular association of the type lone pair···π/π···π/π···anion···π/π···lone pair in **1** is observed, along with the aforementioned O···O short contacts. Similarly to the transition-metal complexes $(C_6H_8N_2H)_2[M(C_3H_2O_4)_2(H_2O)_2]\cdot 4H_2O$ (M = Ni/Co/Mn), a network of lone pair···π interactions is noticed in **2**. In addition, several important aspects of compounds **1** and **2** have been analyzed using theoretical calculations. Since several noncovalent interactions present in the crystal structures are weak and dispersion effects are important to properly describe these interactions, we have used the DFT-D method. We have studied the energetic features of some fragments of the crystal in order to know the importance of the noncovalent interactions observed. We have also characterized them using Bader's theory of atoms-in-molecules,[69] which provides an unambiguous definition of chemical bonding.

Experimental Section

Physical Measurements. IR spectra were recorded on a Perkin-Elmer RXI FT-IR spectrophotometer with the sample prepared as a KBr pellet, in the range 4000−600 cm^{-1}. Elemental analyses (C, H, N) were performed on a Perkin-Elmer 240C elemental analyzer.

Materials. All reactions were carried out in aerobic conditions and with water as the solvent. Malonic acid, magnesium(II) perchlorate hexahydrate, magnesium(II) sulfate heptahydrate, 2-aminopyridine, and 2-amino-4-picoline (all from Aldrich) were used as received. Freshly boiled, doubly distilled water was used throughout the present investigation.

Synthesis of Compound 1. Magnesium(II) perchlorate hexahydrate (0.331 g, 1.0 mmol) dissolved in 25 mL of water was allowed to react with malonic acid (0.208 g, 2.0 mmol) in water (25 mL) at 60 °C, resulting in a clear colorless solution. A warm aqueous solution (20 mL) of 2-aminopyridine (0.376 g, 4.0 mmol) was added dropwise to the above colorless solution with continuous stirring. The pH of the resulting solution was adjusted to 5.5 by the addition of dilute aqueous NaOH. The reaction mixture thus obtained was further heated at 60 °C for an hour with continuous stirring. The solution was then cooled to room temperature and left unperturbed for crystallization. After a few weeks, flat, colorless single crystals suitable for X-ray analysis were obtained. The crystals were collected by filtration, washed with cold water, and dried in air (yield: 48%). Anal. Calcd for $C_{26}H_{36}N_8O_{18}Cl_2Mg$: C, 37.00; H, 4.30; N, 13.27%. Found: C, 36.92; H, 4.25; N, 13.15%. The main IR absorption bands observed for **1** (KBr pellet, cm^{-1}) are the following: 3340 (b), 3147 (w), 2977 (m), 1677 (s), 1633 (m), 1573 (s), 1481 (s), 1434 (s), 1365 (s), 1247 (s), 1116 (m), 1085 (m), 999 (m), 973 (m), 767 (s), 729 (s), 628 (s), 551 (w), 513 (w).

Synthesis of Compound 2. Magnesium(II) sulfate heptahydrate (0.246 g, 1.0 mmol) dissolved in 25 mL of water was allowed to react with malonic acid (0.208 g, 2.0 mmol) in water (25 mL) at 60 °C, resulting in a clear colorless solution. A warm aqueous solution (20 mL) of 2-amino-4-picoline (0.216 g, 2.0 mmol) was added dropwise to the above colorless solution with continuous stirring. The pH of the resulting solution was adjusted to 5.5 by the addition of dilute aqueous NaOH. The reaction mixture thus obtained was further heated at 60 °C for an hour with continuous stirring. The solution was then cooled to room temperature and left unperturbed for crystallization. After a few weeks, flat, colorless single crystals suitable for X-ray analysis were obtained. The crystals were collected by filtration, washed with cold water, and dried in air (yield: 52%). Anal. Calcd for $C_{18}H_{34}N_4O_{14}Mg$: C, 38.96; H, 6.17; N, 10.09%. Found: C, 38.82; H, 6.08; N, 10.01%. The main IR absorption bands observed for **2** (KBr pellet, cm^{-1}) are the following: 3251 (b), 3060 (b), 2850 (w), 1677 (s), 1641 (m), 1593 (s), 1487 (m), 1436 (s), 1361 (vs), 1245 (s), 1164 (s), 798 (s), 717 (s), 568 (s), 513 (s).

X-ray Crystal Structure Determination of 1 and 2. X-ray diffraction data collection was carried out on a Bruker SMART APEX CCD diffractometer with graphite monochromated Mo Kα radiation (λ = 0.71073 Å). The data were processed using SAINT.[70] The crystal structures were solved by direct methods using SHELXS-97[70] and refined by full-matrix least-squares on F^2 with SHELXL-97.[70] Other calculations were carried out using the SHELXTL package.[70] For both complexes, the H atoms other than those bonded to O and N were placed in geometrically idealized positions and constrained to ride on their parent atoms. Hydrogen atoms bonded to oxygen and nitrogen atoms were found by difference Fourier methods and refined isotropically.

Theoretical Methods. The geometries of all complexes studied in this work were computed at the RI-B97-D/TZVP level of theory using the program TURBOMOLE version 5.7.[71] The RI-DFT method applied to the study of weak interactions is considerably faster than the DFT approach, and the interaction

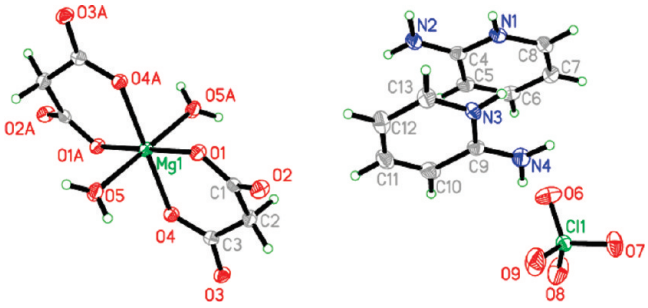

Figure 1. ORTEP diagram of complex **1** with atom-numbering scheme. The thermal ellipsoids are drawn at the 50% probability level. Atoms marked with "A" are generated by the inversion operation ($-x$, $2 - y$, $-z$).

TABLE 1: Crystallographic Data for Compounds 1 and 2

compound	1	2
formula	$C_{26}H_{36}N_8O_{18}Cl_2Mg$	$C_{18}H_{34}N_4O_{14}Mg$
M (g mol^{-1})	843.84	554.80
crystal system	triclinic	triclinic
space group	$P\bar{1}$ (no. 2)	$P\bar{1}$ (no. 2)
a (Å)	7.1460(9)	7.534(3)
b (Å)	11.1812(14)	9.052(4)
c (Å)	11.6020(14)	10.428(4)
α (deg)	88.373(2)	93.370(8)
β (deg)	81.837(2)	93.118(8)
Γ (deg)	74.342(2)	112.237(7)
F(000)	438	294
V (Å^3)	883.52(19)	654.9(5)
Z	1	1
T/K	100	100
theta min−max (deg)	1.8−26.3	2.0−25.0
λ (Mo Kα) (Å)	0.71073	0.71073
μ (Mo Kα) (mm^{-1})	0.292	0.142
crystal size (mm^3)	0.30 × 0.50 × 0.50	0.25 × 0.25 × 0.40
$R1$, $I > 2\sigma(I)$ (all)	0.0443	0.0529
w$R2$, $I > 2\sigma(I)$ (all)	0.1109	0.1388
S(GOF)	1.06	1.00
total reflections	6955	3265
independent reflections (R_{int})	3507 (0.059)	2260 (0.061)
observed data [$I > 2\sigma(I)$]	3208	1736
min and max resd dens (e/Å^3)	−0.60, 0.88	−0.39, 0.35

energies and equilibrium distances are almost identical for both methods.[72] The AIM analysis[69] of the different crystal fragments has been performed by means of the AIM2000 version 2.0 program[73] using the BB95/TZVP wave function and the geometry obtained from the crystallographic coordinates.

Results and Discussion

Crystal Structure Description of 1. Compound **1** crystallizes in the triclinic space group $P\bar{1}$ with the asymmetric unit consisting of half of the molecular anion $[Mg(C_3H_2O_4)_2(H_2O)_2]^{2-}$, two crystallographically independent $C_5H_7N_2^+$ (protonated 2-aminopyridine) cations, and a perchlorate anion. The full anion is generated by the symmetry operation of an inversion center. A representative ORTEP diagram is shown in Figure 1. Crystallographic data collection and refinement parameters, selected bond lengths and angles, and supramolecular interactions are listed in Tables 1, 2, and 3, respectively.

The magnesium(II) ion, located on an inversion center, is in an octahedral coordination environment whose equatorial plane is formed by the oxygen atoms O1 and O4 from one malonate unit and their symmetry related counterparts O1A, O4A (A = $-x$, $2 - y$, $-z$) from a second malonate unit. Two water

TABLE 2: Selected Bond Lengths (Å) and Angles (deg) for 1

Mg(1)−O(1)	2.0260(15)	O(4)−C(3)	1.274(3)
Mg(1)−O(4)	2.0056(13)	O(3)−C(3)	1.233(2)
Mg(1)−O(5)	2.0951(16)	C(1)−C(2)	1.521(3)
O(1)−C(1)	1.263(3)	C(2)−C(3)	1.522(3)
O(2)−C(1)	1.246(3)		
O(1)−Mg(1)−O(4)	88.71(6)	Mg(1)−O(4)−C(3)	131.52(13)
O(1)−Mg(1)−O(5)	87.33(6)	O(4)−C(3)−O(3)	123.56(19)
O(1)−Mg(1)−O(4)[a]	91.29(6)	C(1)−C(2)−C(3)	120.78(17)
O(1)−Mg(1)−O(5)[a]	92.67(6)	O(1)−C(1)−O(2)	122.75(18)
O(4)−Mg(1)−O(5)	86.52(6)	O(4)−C(3)−C(2)	119.50(17)
O(4)−Mg(1)−O(5)[a]	93.48(6)	O(1)−C(1)−C(2)	119.78(19)
Mg(1)−O(1)−C(1)	130.10(13)	O(4)−C(3)−C(2)	119.50(17)

[a] Symmetry code: $-x$, $2 - y$, $-z$.

molecules (O5 and O5A, A = $-x$, $2 - y$, $-z$) occupy the *trans* axial positions, thus generating a $MgO_4O'_2$ chromophore. The Mg−O bond distances in the equatorial plane vary between 2.0056(13) and 2.0260(15) Å, and the angle subtended at the Mg atom by the malonate ligand is 88.71(6)°. The value of the apical Mg(1)−O(5) bond length is 2.0951(16) Å. These bond lengths and angles are similar to those found in our recently reported complex $(C_5H_7N_2)_4[Mg(mal)_2(H_2O)_2](NO_3)_2$ [mal = $C_3H_2O_4$ = malonate dianion; $C_5H_7N_2$ = protonated 2-aminopyridine],[44] and comparable to those of related Mg complexes described in the literature,[74–79] as well as malonate moieties.[80]

The monomeric anionic units $[Mg(C_3H_2O_4)_2(H_2O)_2]^{2-}$ are interlinked to each other *via* strong self-complementary O5−H5OA···O2 hydrogen bonds, which give rise to an $R_2^2(12)$ motif. This assembly generates an infinite 1D chain along the crystallographic a axis (Figure 2). Each monomeric anionic unit also recognizes four aminopyridinium cations ($C_5H_7N_2^+$) through doubly coordinated carboxylate ends, leading to $R_2^2(8)$ hydrogen-bonding synthons (Figure 2), involving the hydrogen bonds N2−H2NB···O2, N1−H1N···O1 and N4−H4NB···O3, N3−H3N···O4. Two dangling perchlorate ions are also attached to each monomeric unit by O5−H5OB···O7 hydrogen bonds. These perchlorate anions play a pivotal role in the construction of 2D sheets involving $[Mg(C_3H_2O_4)_2(H_2O)_2]^{2-}$ units (Figure 3). These 2D sheets form the [011] plane of the crystal lattice. In these 2D sheets, unusual short contacts between oxygen atoms (O9) of lattice perchlorate anions are observed. The distance between two O9 atoms is 2.803(3) Å, which is much shorter than the sum of their corresponding van der Waals radii (rvdW: O, 1.52 Å). As the theoretical calculations revealed these O···O interactions in this system to be repulsive (see below), strong hydrogen-bonding intractions among the various charged components, along with anion···π interactions, most likely force the perchlorate anions to come close enough to exhibit such an unusual contact between the oxygen (O9) atoms.

The noncoordinating O3 atom is orientated toward the π-face of a 2-aminopyridine moiety (Figure 2). The distance between O3 and the centroid of the aminopyridine ring is 3.2104(18) Å [angle α = C3−O3···Cg(1) = 130.96(14)°, C3···Cg(1) = 4.125(2) Å, where Cg(1) is the centroid of the ring, defined by the atoms N(1)/C(4)/C(5)/C(6)/C(7)/C(8)]. In this case, the carbonyl oxygen (O3) approaches the π-face of the aminopyridine ring with an angle of 130.96(14)°, suggesting a significant lone pair···π interaction.[36,43,44] The shortest separation distance reflecting this interaction is O3···C4 = 2.976(3) Å, which is below the sum of the corresponding van der Waals radii (the sum of van der Waals radii of O and C is 3.22 Å).[81] This 2-aminopyridine ring is further stacked over a second aminopy-

TABLE 3: Relevant H-Bonds in Compound 1

D−H···A	D−H (Å)	H···A (Å)	D···A (Å)	D−H···A (deg)	symmetry
O5−H5OA···O2	0.84(4)	1.85(4)	2.677(2)	169(3)	$1-x, 2-y, -z$
N1−H1N···O1	0.85(2)	1.99(2)	2.835(2)	174(2)	$1-x, 1-y, -z$
O5−H5OB···O7	0.82(3)	2.00(2)	2.813(2)	173(3)	$-1+x, 1+y, -1+z$
N2−H2NA···O8	0.87(3)	2.29(3)	3.095(3)	154(2)	$1-x, 1-y, 1-z$
N3−H3N···O4	0.85(3)	1.93(3)	2.773(2)	173(3)	$1+x, -1+y, z$
N2−H2NB···O2	0.86(3)	2.04(3)	2.893(2)	169(3)	$1-x, 1-y, -z$
N4−H4NA···O6	0.91(3)	2.49(3)	3.255(3)	143(3)	
N4−H4NA···O9	0.91(3)	2.41(3)	3.266(3)	158(3)	
N4−H4NB···O3	0.87(3)	1.97(3)	2.829(3)	175(2)	$1+x, -1+y, z$
C2−H2C···O6	0.9900	2.4300	3.384(3)	163	$1-x, 1-y, 1-z$
C7−H7···O3	0.9500	2.4800	3.413(3)	165	$1-x, 1-y, 1-z$
C13−H13···O8	0.9500	2.4700	3.243(3)	139	$x, y, -1+z$

ridine molecule [R(1) = N(1)/C(4)/C(5)/C(6)/C(7)/C(8); R(2) = N(3)/C(9)/C(10)/C(11)/C(12)/C(13); symmetry code x, y, z]. The centroid-to-centroid distance is 4.2521(13) Å, and the dihedral angle amounts to 11.83°. The amino nitrogen atoms N2 and N4 lie only 3.46 and 3.29 Å above the π face of the parallel stacked 2-aminopyridine rings, revealing an unusual stacking of the $-NH_2$ group over the aromatic-π cloud. These coupled lone pair$\cdots\pi$ and $\pi\cdots\pi$ interactions within the monomeric units add stability to the formation of the 1D tape (Figure 2). One perchlorate anion from an adjacent monomeric unit along the *a* axis is sandwiched between two aminopyridine rings through anion$\cdots\pi$ contacts involving the oxygen atoms O9 and O6, leading to a $\pi\cdots$anion$\cdots\pi$ type interaction. The shortest separation distances reflecting these interactions are O9···C10 = 3.150(3) Å and O6···C6 = 3.085(3) Å, which are below the sum of the corresponding van der Waals radii (the sum of van der Waals radii of O and C is 3.22 Å).[81] The aminopyridine ring which is in anion$\cdots\pi$ contact with the atom O6 of a perchlorate anion is further interacting with the oxygen atom O3 of a malonate moiety, generating an additional lone pair$\cdots\pi$ association. Therefore, this entire assembly as a whole produces a rare supramolecular combination of lone pair$\cdots\pi$, $\pi\cdots\pi$, and anion$\cdots\pi$ interactions, which can be designated as a lone pair$\cdots\pi/\pi\cdots\pi/\pi\cdots$anion$\cdots\pi/\pi\cdots$lone pair network (Figure 4). This association illustrates the occurrence of an elegant combination of weak forces in the solid-state structure of a metal−organic hybrid complex, which contributes to the self-assembly process. This network appears to be responsible for the overall three-dimensional packing of the complex.

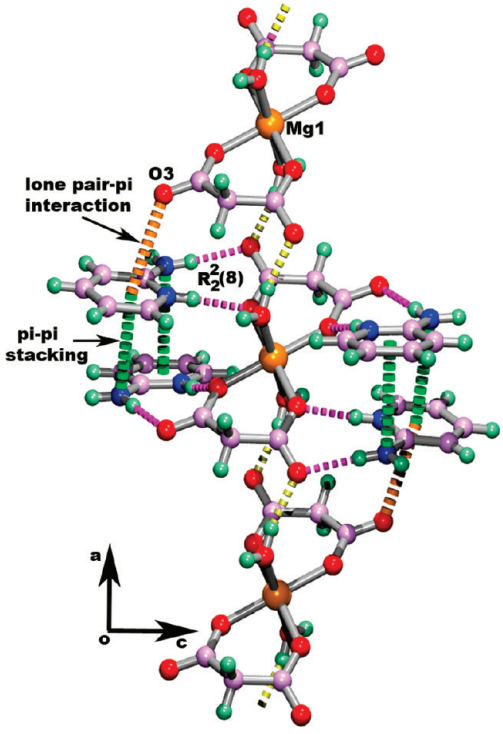

Figure 2. Formation of a 1D chain in **1** through the association of discrete $[Mg(mal)_2(H_2O)_2]^{2-}$ monomeric units. The chain is viewed along the *b* axis. The occurrence of hydrogen-bonding interactions (O5−H5OA···O2) along the *a* axis generates an $R_2^2(12)$ cyclic motif. Each monomeric unit is also connected to four 2-aminopyridinium cations. The perchlorate anions and other aminopyridinium cations are omitted for clarity. Color code: Mg, orange; O, red; N, blue; C, light purple; H, aquamarine.

Crystal Structure Description of 2. Compound **2** also crystallizes in the triclinic space group $P\bar{1}$ with the asymmetric unit consisting of half of the molecular anion $[Mg(C_3H_2O_4)_2(H_2O)_2]^{2-}$, one $C_6H_8N_2H^+$cation, and two lattice water molecules. The anionic unit is centrosymmetric with the metal atoms occupying a center of inversion. A representative ORTEP diagram is shown in Figure 5, while crystallographic data collection and refinement parameters, selected bond lengths, angles, and supramolecular interactions are listed in Tables 1, 4, and 5, respectively.

Two oxygen atoms (O1 and O2) from one didentate malonate moiety and their centrosymmetric counterparts (O1A and O2A, A = $-x, -y, -z$) of a symmetry-related malonate unit constitute the equatorial plane of the octahedrally bound Mg atoms. Two water molecules occupy the *trans* axial positions, thus generating a $MgO_4O'_2$ chromophore. The Mg−O bond distances in the equatorial plane vary between 2.028(2) and 2.089(2) Å, and the angle subtended at the Mg atom by the malonate ligand is 88.54(7)°. The value of the apical Mg(1)−O(5) bond length is 2.063(3) Å. In compound **2**, the equatorial bonds are elongated, while the axial bonds are compressed compared to our recently reported complex $(C_5H_7N_2)_4[Mg(mal)_2(H_2O)_2](NO_3)_2$ [mal = $C_3H_2O_4$ = malonate dianion; $C_5H_7N_2$ = protonated 2-aminopyridine].[44] However, these bond lengths and angles are comparable to related magnesium compounds found in the literature.[74–79] Malonate ligands usually adopt an envelope conformation in which only the methylene group is significantly displaced from the chelate ring plane,[43,44] and the present example is also in line with this generalization. The bond lengths and angles for the metal-chelated malonato moieties are comparable to those previously reported for transition-metal complexes.[80]

The monomeric $[Mg(mal)_2(H_2O)_2]^{2-}$ units are interlinked to each other through the hydrogen bonds (O5−H1O···O7 = 2.747(3) Å and O5−H2O···O7 = 2.743(3) Å, see Table 5 for the hydrogen-bonding parameters), forming a supramolecular chain along the *a* axis. The coordinated water molecules (O5)

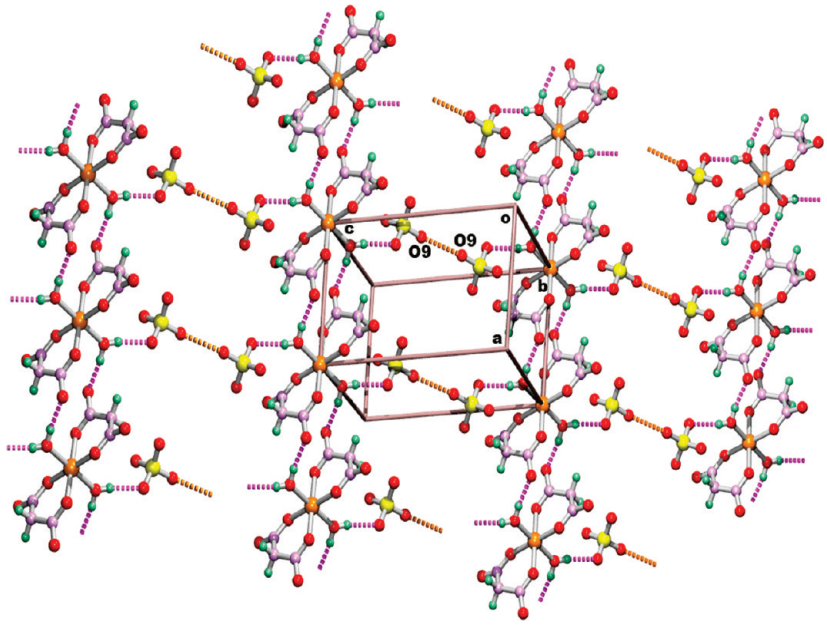

Figure 3. Formation of a 2D supramolecular sheet in **1** through O9···O9 [2.803(3) Å] short contacts. 2-Aminopyridinium cations have been omitted for clarity. Color code: Mg, orange; O, red; C, light purple; H, aquamarine: Cl, yellow.

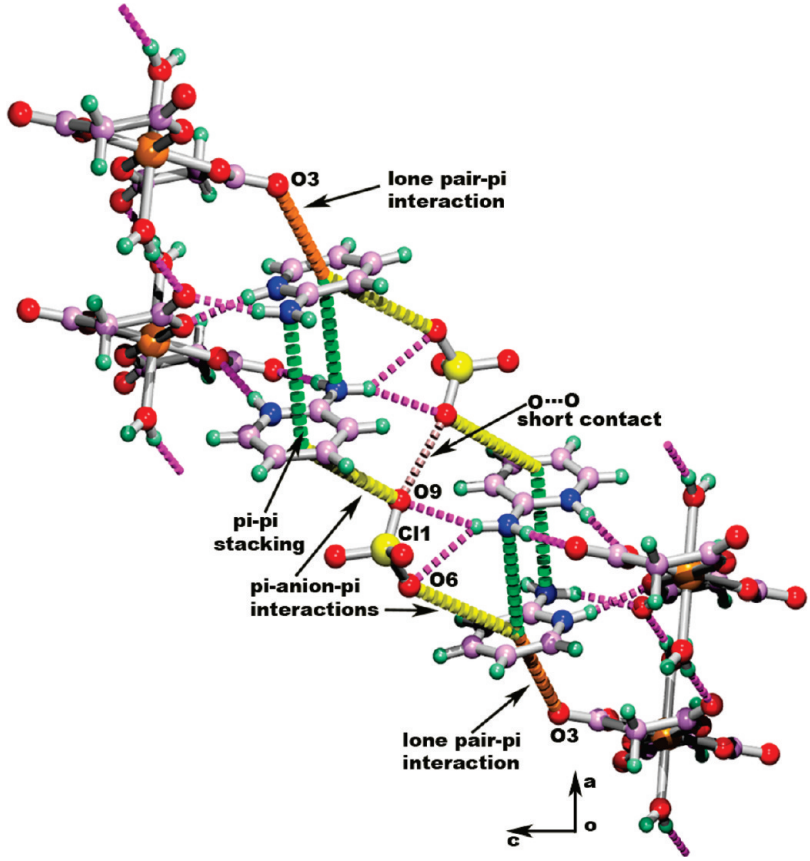

Figure 4. Supramolecular network in **1**, generated through lone pair···π/π···π/π···anion···π/lone pair···π interactions. Color code: Mg, orange; O, red; N, blue; C, light purple; H, aquamarine; Cl, yellow.

from successive $[Mg(mal)_2(H_2O)_2]^{2-}$ anions and lattice water molecules (O7 along with its symmetry related counterpart O7*; * = $-x$, $-y$, $-z$) form a tetrameric water cluster (Figure 6). Each such chain is linked to adjacent chains by means of hydrogen-bonding contacts, which generate a 2D metal-malonate layer in the *ab* plane (Figure 6). These supramolecular interactions give rise to a shifting of the successive chains, by *a*/2 with respect to each other, to facilitate the hydrogen bonding of the malonate (O4) atom at the other corner of the water tetramer, where O7 acts as a donor for O4, thus producing a supramolecular layer (Figure 6).

The 3D supramolecular self-assembly in the solid-state structure of **2** can be regarded as the stacking of successive metal−organic and organic layers. 2-Amino-4-picolinium cations constituting the organic layer are sandwiched between metal-malonate layers. The 2-amino-4-picolinium cations are

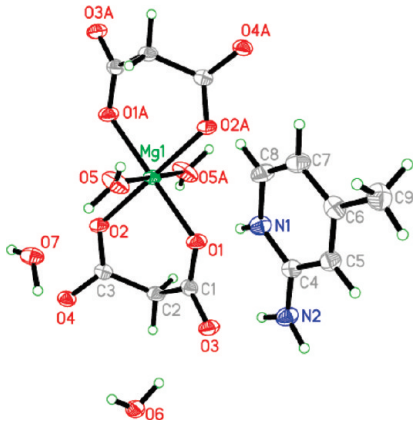

Figure 5. ORTEP diagram of complex **2** with atom-numbering scheme. The thermal ellipsoids are drawn at the 50% probability level. Atoms marked with "A" are generated by the inversion operation ($-x$, $-y$, $-z$).

TABLE 4: Selected Bond Lengths (Å) and Angles (deg) for 2

Mg(1)−O(1)	2.089(2)	O(4)−C(3)	1.258(3)
Mg(1)−O(2)	2.0276(19)	O(3)−C(1)	1.250(4)
Mg(1)−O(5)	2.063(3)	C(1)−C(2)	1.514(4)
O(1)−C(1)	1.277(3)	C(2)−C(3)	1.523(4)
O(2)−C(3)	1.270(3)		
O(1)−Mg(1)−O(2)	88.54(7)	Mg(1)−O(2)−C(3)	128.85(19)
O(1)−Mg(1)−O(5)	86.80(9)	O(2)−C(3)−O(4)	123.1(3)
O(1)−Mg(1)−O(2)[a]	91.46(7)	C(1)−C(2)−C(3)	115.1(2)
O(1)−Mg(1)−O(5)[a]	93.20(9)	O(1)−C(1)−O(3)	123.7(3)
O(2)−Mg(1)−O(5)	88.42(10)	O(4)−C(3)−C(2)	118.9(2)
O(2)−Mg(1)−O(5)[a]	91.58(10)	O(1)−C(1)−C(2)	118.1(3)
Mg(1)−O(1)−C(1)	126.52(18)	O(2)−C(3)−C(2)	118.0(2)

[a] Symmetry code: $-x$, $-y$, $-z$.

attached to the layer from either side and bind to the malonate terminals through the formation of the characteristic $R_2^2(8)$ recognition motif (Figure 7). The binding of the 2-amino-4-picolinium cations to the layer is further strengthened by an additional C−H···O hydrogen bond with the nearest oxygen atom of the adjacent malonate terminal across the metal, forming a $R_2^2(7)$ supramolecular pattern (Figure 7). These two motifs act together, and a tripodal recognition of the 2-amino-4-picolinium cations enhances the stability of the supramolecular assembly.[68] Successive 2-amino-4-picolinium-studded layers pack along the crystallographic *c* axis through interdigitation, which is primarily facilitated by $\pi\cdots\pi$ interactions [R(1) = N(1)/C(4)/C(5)/C(6)/C(7)/C(8), centroid···centroid distance of 3.994(2) Å, symmetry code: $1-x$, $-y$, $1-z$, dihedral angle = 0°, the angle between the centroid−centriod joining line and the normal from the first ring center to the second ring plane is 26.66°, slippage = 1.792 Å] between the 2-amino-4-picolinium moieties attached to adjacent layers (Figure 8).

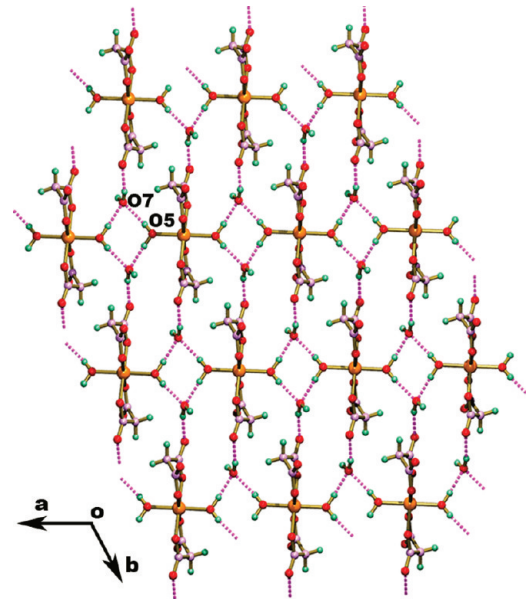

Figure 6. Organization of the monomeric $[Mg(mal)_2(H_2O)_2]^{2-}$ units of **2** into a 2D layer in the *ab* plane in which the water tetramer acts as a supramolecular synthon. 2-Amino-4-picolinium cations have been omitted for clarity. Color code: Mg, orange; O, red; C, light purple; H, aquamarine.

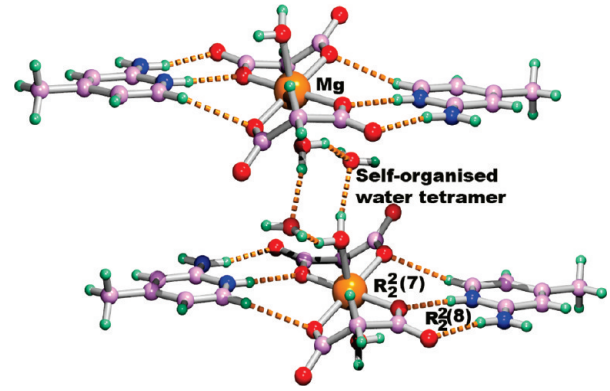

Figure 7. Tripodal recognition between protonated 2-amino-4-picolinium cations and malonate moieties in **2**, through the formation of $R_2^2(8)$ and $R_2^2(7)$ hydrogen-bonding motifs on both sides of the water-assembled layer. Color code: Mg, orange; O, red; N, blue; C, light purple; H, aquamarine.

A close examination of the weak forces in the Mg(II) complex **2** reveals the presence of two possible salt-bridge···π interactions which will be described in detail below. This type of interactions has been described in the literature;[82] they are important in biological systems. In addition to these forces, hydrogen-bonding and $\pi\cdots\pi$ stacking interactions are present (see Figure 9).

TABLE 5: Relevant H-Bonds in Compound 2

D−H···A	D−H (Å)	H···A (Å)	D···A (Å)	D−H···A (deg)	symmetry
N1−H1N···O1	0.81(3)	2.04(3)	2.841(4)	176(3)	
O5−H1O···O7	0.93(5)	1.82(4)	2.747(3)	174(4)	
N2−H2N···O3	0.93(4)	1.87(4)	2.793(4)	171(3)	
O5−H2O···O7	0.82(4)	1.95(4)	2.743(3)	164(4)	$1-x$, $-y$, $-z$
N2−H3N···O6	0.92(3)	1.91(3)	2.836(4)	176(3)	$1-x$, $1-y$, $1-z$
O6−H3O···O4	0.75(4)	1.98(4)	2.728(3)	172(4)	$1-x$, $1-y$, $-z$
O6−H4O···O3	0.89(4)	1.90(4)	2.786(3)	179(5)	
O7−H5O···O4	0.87(4)	1.87(4)	2.710(3)	164(5)	$1-x$, $1-y$, $-z$
O7−H6O···O6	0.96(4)	1.82(4)	2.765(3)	165(3)	$1-x$, $1-y$, $-z$
C8−H8···O2	0.95	2.5500	3.269(4)	133	$-x$, $-y$, $-z$

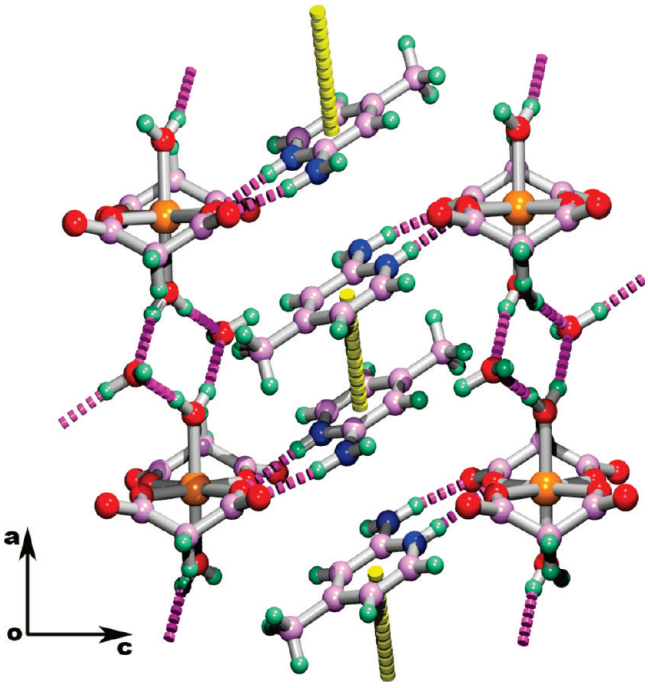

Figure 8. View (through the *b* axis) of the interdigitation of organic layers in **2**, by means of $\pi\cdots\pi$ interactions along the crystallographic *c* axis. Color code: Mg, orange; O, red; N, blue; C, light purple; H, aquamarine.

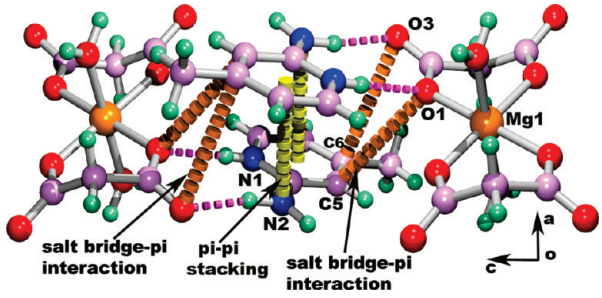

Figure 9. Occurrence of significant salt bridge$\cdots\pi$ interactions in **2**, involving the carboxylate oxygen (shown by coral) atoms O1 and O3. Color code: Mg, orange; O, red; N, blue; C, light purple; H, aquamarine.

Although in recent years, supramolecular chemists are more and more interested in unraveling the individual potentiality of two particular weak forces, namely, the anion$\cdots\pi$ and lone pair$\cdots\pi$ interactions (contrary to the intuitive expectation that such interactions are repulsive), an exciting aspect is still in a state of infancy, that is, the associative interactions of such forces (i.e., lone pair$\cdots\pi/\pi\cdots\pi/\pi\cdots$lone pair and lone pair$\cdots\pi/\pi\cdots\pi$/anion$\cdots\pi$) to form extended networks and their supramolecular consequences in the solid state. Such coupling of weak forces has been primarily observed while examining the self-assembly of some transition-metal− and non-transition-metal−organic hybrid complexes, namely, $(C_6H_8N_2H)_2$-$[Ni(ntaH)_2]$[43] (**3**), $(C_5H_7N_2)_2[Cu(mal)_2(H_2O)_2]$[43] (**4**), $(C_5H_7N_2)_4$-$[Ni(mal)_2(H_2O)_2](NO_3)_2$[43] (**5**), and $(C_5H_7N_2)_4[Mg(mal)_2(H_2O)_2]$-$(NO_3)_2$[44] (**6**) [$ntaH_3$ = nitrilotriacetic acid; $C_6H_8N_2H$ = protonated 2-amino-4-picoline; $malH_2$ = malonic acid; $C_5H_7N_2$ = protonated 2-aminopyridine], and exploring their intriguing role in the crystal packing. These interactions were also investigated by density functional theory studies, which clearly revealed the favorable formation of such unique combinations. A simple change in counteranion, i.e., from nitrate to perchlorate, yielded complex **1**, which is similar in formulation with **6**, but significant differences in the self-assembly process are observed. The consolidation of the 2D sheets through a combination of noncovalent O$\cdots$O, anion$\cdots\pi$, and hydrogen-bonding interactions, involving the oxygen atom O9 from lattice perchlorate ions, is indeed a unique feature found in **1**. In **6**, the combined interactions lone pair$\cdots\pi/\pi\cdots\pi/$anion$\cdots\pi$ are responsible for the 2D assembly. The network in **1** is further extended by the perchlorate anions, whose oxygen atoms O6 and O9 are involved in additional anion$\cdots\pi$ bonding contacts, which generate an intricate network of weak forces of the type lone pair$\cdots\pi/\pi\cdots\pi/\pi\cdots$anion$\cdots\pi/\pi\cdots$lone pair, responsible for the overall 3D packing in **1**. Interestingly, in **6**, hydrogen bonds direct the 3D packing of the complex. Therefore, the comparative analysis of the structural features observed for **1** and **6** reveals that a simple change in counteranion gives rise to unpredictable, significant differences in the crystal packing of compounds with close formulations. It is also noteworthy that the basic features of the self-assembly process of **1** and **6** are similar, that is, the formation of monomeric anionic units $[Mg(mal)_2(H_2O)_2]^{2-}$ which assemble to generate a 1D chain through an $R^2_2(12)$ hydrogen-bonding synthon, and the recognition of the 2-aminopyridinium cations by the monomeric units through the formation of an $R^2_2(8)$ hydrogen-bonding motif. However, the involvement of different weak dispersive forces in the respective crystal packing of **1** and **6** causes significant structural changes, since a 2D supramolecular network is observed for **1**, while **6** exhibits a 3D arrangement. This system has been further investigated by examining the effect on the crystal structure of the replacement of 2-aminopyridine by 2-amino-4-picoline. The resulting compound **2** is found to be isostructural with previously reported transition-metal complexes, thus suggesting the robustness and effectiveness of the supramolecular energy contribution to the stabilization of these complexes in the solid state. This apparently emerges from the fact that solvent water molecules are in synergistic combination with the metal-malonate framework and the weak dispersive forces ($\pi\cdots\pi$ and lone pair$\cdots\pi$ interactions) to facilitate the organization of individual coordination monomers, through their inherent tendency to self-assemble into tetrameric water clusters. Irrespective of the metal ions present (transition-metal or non-transition-metal ion), this assembly remains unperturbed.

Theoretical Study. We have divided the theoretical study into two parts. First, for each compound, we have computed a large fragment of the crystal structure where all representative noncovalent interactions are present. We have obtained the distribution of critical points that characterizes each of these interactions. Second, we have computed the interaction energies of some models of the crystal structures to further study the assemblies observed in the solid state. We have also analyzed the unusual O$\cdots$O interactions and the special $\pi-\pi$ interaction between the 2-aminopyridine rings that reveals an atypical stacking of the $-NH_2$ group over the aromatic-π cloud. Before presenting the results, some considerations should be made. We have studied several fragments of the crystal, which have been carefully chosen to be neutral. This is important in order to be as realistic as possible, since the utilization of charged systems may influence the strength of the interactions. Obviously, the compound is neutral; however, it is composed of several charged subunits, namely, perchlorate anion, $[Mg(C_3H_2O_4)_2(H_2O)_2]^{2-}$ dianion, and protonated 2-aminopyridine. The $[Mg(C_3H_2O_4)_2(H_2O)_2]^{2-}$ dianion has been used to adjust the charge in several fragments, replacing a bidentate malonate ligand by a monodentate formate ligand and a water molecule. This approximation is supported by the

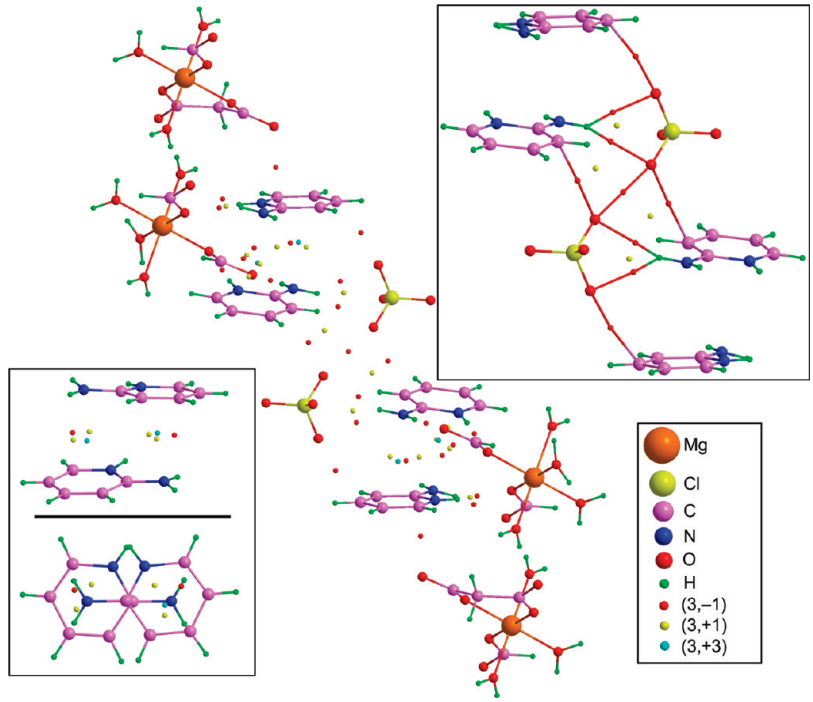

Figure 10. AIM analysis of a large fragment of compound **1**.

fact that each $[Mg(C_3H_2O_4)_2(H_2O)_2]^{2-}$ dianion interacts with two sets of stacked 2-aminopyridine moieties (see Figure 2, central anion) and in the crystal fragment in which we have chosen to perform the theoretical study only one set is used. In addition, it should be mentioned that the strongest noncovalent interactions present in the solid state are found between charged ions. Furthermore, hydrogen-bonding interactions are also very important for the formation of the supramolecular networks. Nevertheless, the influence of other less studied weak interactions, as the ones reported in this manuscript, on the crystal architecture is also essential. Therefore, its analysis is of great importance to explain the supramolecular assembly of the complexes reported here.

The AIM analysis of a large fragment of the crystal structure of compound **1** is shown in Figure 10. It can be observed that all previously described noncovalent interactions are characterized by the presence of several critical points (CPs). In Figure 10, we have included only the CPs that characterize the hydrogen-bonding, $\pi\cdots\pi$, lone pair$\cdots\pi$, and anion$\cdots\pi$ interactions. The other CPs have been omitted for the sake of clarity. The lone pair$\cdots\pi$ interaction involving the carboxylic oxygen atom of the malonate ligand is characterized by the presence of a bond CP connecting the oxygen atom and one carbon atom of the ring. In the top-right part of Figure 10, we have highlighted the interactions involving the ClO_4^- ion, omitting the other CPs. The bond paths are represented in this part of the figure. It can be observed that one hydrogen atom of the amino group establishes a bifurcated H-bond with the anion, which is characterized by two-bond (red sphere) and one-ring (yellow sphere) CPs. Moreover, each perchlorate ion participates in two displaced anion$\cdots\pi$ interactions using two different oxygen atoms. This $\pi\cdots$anion$\cdots\pi$ interaction is characterized by two bond CPs that connect each oxygen atom with an aromatic carbon atom. Finally, a bond CP connecting two oxygen atoms of two different anions is also observed, confirming the unusual O$\cdots$O interaction. The AIM analysis of the $\pi\cdots\pi$ stacking interaction between the two 2-aminopyridine rings is highlighted at the bottom-left part of Figure 10. From the on-top view, it can be observed that the interaction can be better described as two lone pair$\cdots\pi$ interactions between the nitrogen atom of the $-NH_2$ group of one moiety and the pyridine ring of the other. In fact, a cage CP (light-blue sphere) connects the nitrogen atom to the center of the ring. The presence of this type of CP is characteristic of lone pair$\cdots\pi$ interactions.

The noncovalent interactions described in the Experimental Section have been confirmed by means of the AIM analysis. The presence of a bond CP connecting two atoms implies an interaction and a positive sign of the Laplacian of the charge density at the bond CPs and suggests a closed-shell nature of the interaction. However, it does not imply a favorable interaction, since it can be repulsive. Therefore, an energetic analysis should be performed to determine whether the interaction is favorable or unfavorable. This is especially true in compound **1**, where the O$\cdots$O interaction is established between two oxygen atoms belonging to an anionic species, and therefore a repulsive interaction is expected. In an attempt to study the energy characteristics of this interaction, we have performed DFT-D calculations on a neutral model system denoted as **Q** in Figure 11. This quaternary complex, which is very important in the solid state, is formed by two anion$\cdots\pi$ interactions, two bifurcated hydrogen-bonding interactions, and one O$\cdots$O interaction. Hence, the binding energy of this complex, computed from the monomeric species ($E_{hb+a\pi+oo}$, see Figure 11), accounts for the energetics of the three noncovalent interactions. In addition, the quaternary complex (**Q**) can be obtained by dimerization of the binary complex (**B**[1]), where the hydrogen-bonding interaction has been previously formed. The dimerization energy ($E_{a\pi+oo}$) determines the strength of the anion$\cdots\pi$ and O$\cdots$O interactions. Similarly, the dimerization energy (E_{hb+oo}) of the binary complex (**B**[2]) to produce **Q**, whose anion$\cdots\pi$ interaction has been previously formed, determines the strength of the hydrogen-bonding and O$\cdots$O interactions. The computed $E_{hb+a\pi+oo}$ energy at the RI-B97-D/TZVP level of theory is -182 kcal mol^{-1}, indicating that the overall interaction energy of the quaternary complex starting from the monomers is highly favorable. Remarkably, both dimerization

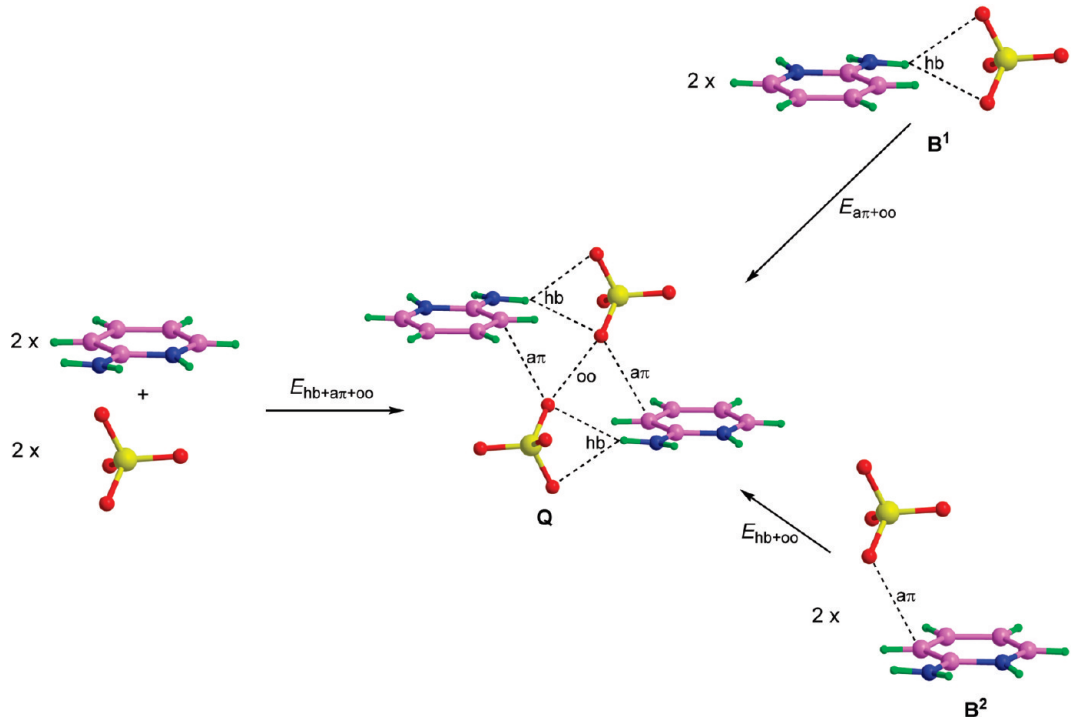

Figure 11. Schematic representation of the quaternary complex (**Q**) and the three different interaction energies considered to evaluate the components.

energies, E_{hb+oo} and $E_{a\pi+oo}$, are very similar, i.e., respectively, −25.59 and −25.18 kcal mol^{-1}, thus indicating that the contribution of the anion$\cdots\pi$ interaction to the binding energy is similar to the contribution of the hydrogen-bonding interaction. This is probably due to the dominance of electrostatic effects in these interactions, since both are established between counterions. A rough estimation of the O$\cdots$O interaction energy (denoted as E_{oo}) can be given using the three binding energies defined in Figure 11. The $E_{hb+a\pi+oo}$ energy reflects the contribution of the three noncovalent interactions to the binding energy of the quaternary complex (**Q**). E_{hb+oo} accounts for the contribution of the hydrogen-bonding and O$\cdots$O interactions, and $E_{a\pi+oo}$ symbolizes the contribution of the anion$\cdots\pi$ and O$\cdots$O interactions. Therefore, the contribution of the O$\cdots$O interaction is $E_{oo} = E_{hb+oo} + E_{a\pi+oo} - E_{hb+a\pi+oo}$. This gives a positive interaction energy of 131.23 kcal mol^{-1}, indicating that the O$\cdots$O interaction in this system is repulsive. This result is reasonable taking into account that there is an important electrostatic repulsion between both anions. This value is probably overestimated, since the presence of other entities in the solid state interacting with the perchlorate anions will result in a weakening of the O$\cdots$O interaction. Moreover, even though this interaction is repulsive, the combination of the three noncovalent interactions gives rise to a very negative binding energy, indicating that this arrangement is a strong binding motif in the crystal packing.

We have studied two interesting characteristics observed in the solid-state structure of compound **2**. First, we have analyzed energetically the tetrameric water cluster (see Figure 6) that appears to be crucial to generate the *ab* plane. Second, some special features of the stacked aminopicoline rings are studied, including a possible salt-bridge$\cdots\pi$ interaction. Regarding the tetrameric water cluster, we have investigated the influence of the metal on the strength of the hydrogen-bonding interaction. It can be observed from the crystal structure that two opposite water molecules of the cluster are coordinated to a magnesium atom. We have computed the binding energy of the tetrameric

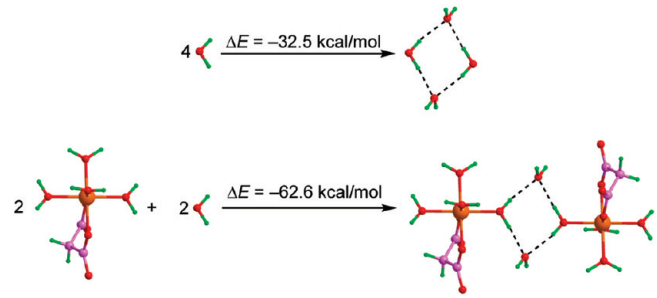

Figure 12. Influence of the metal coordination on the binding energy of the water tetramer.

water cluster, which is −32.5 kcal mol^{-1} (see Figure 12). Thus, the energy of each hydrogen bond is approximately 8 kcal mol^{-1}. In the bottom of Figure 12, we also show the pathway applied to evaluate the influence of the metal on the hydrogen-bonding strength. It should be noted that we have used a neutral model of the $[Mg(mal)_2(H_2O)_2]^{2-}$ anion by replacing one didentate malonate ligand by two water molecules. It can be observed that the coordination of the water molecules to the metal center has a very positive influence ($\Delta E = -62.6$ kcal mol^{-1}) on their ability to form hydrogen bonds, as donors.

From the theoretical study of the 2-aminopyridine stacking in compound **1**, we have concluded that it can be described as a double lone pair$\cdots\pi$ interaction, which is most likely enhanced by the fact that the rings are positively charged. In compound **2**, apparently the stacking of the 2-amino-4-picoline rings is similar. However, there is a significant difference, since the hydrogen-bonding pattern between the $[Mg(mal)_2(H_2O)_2]^{2-}$ anion and the protonated 2-amino-4-picoline ring resembles a salt-bridge. It has been demonstrated[82] that the formation of a salt bridge is enhanced when situated near the face of an aromatic ring. Moreover, the presence of the anion is also important to counteract the *a priori* repulsive electrostatic interaction between two stacked 2-amino-4-picolinium cations. The AIM analyses of two neutral fragments of the crystal

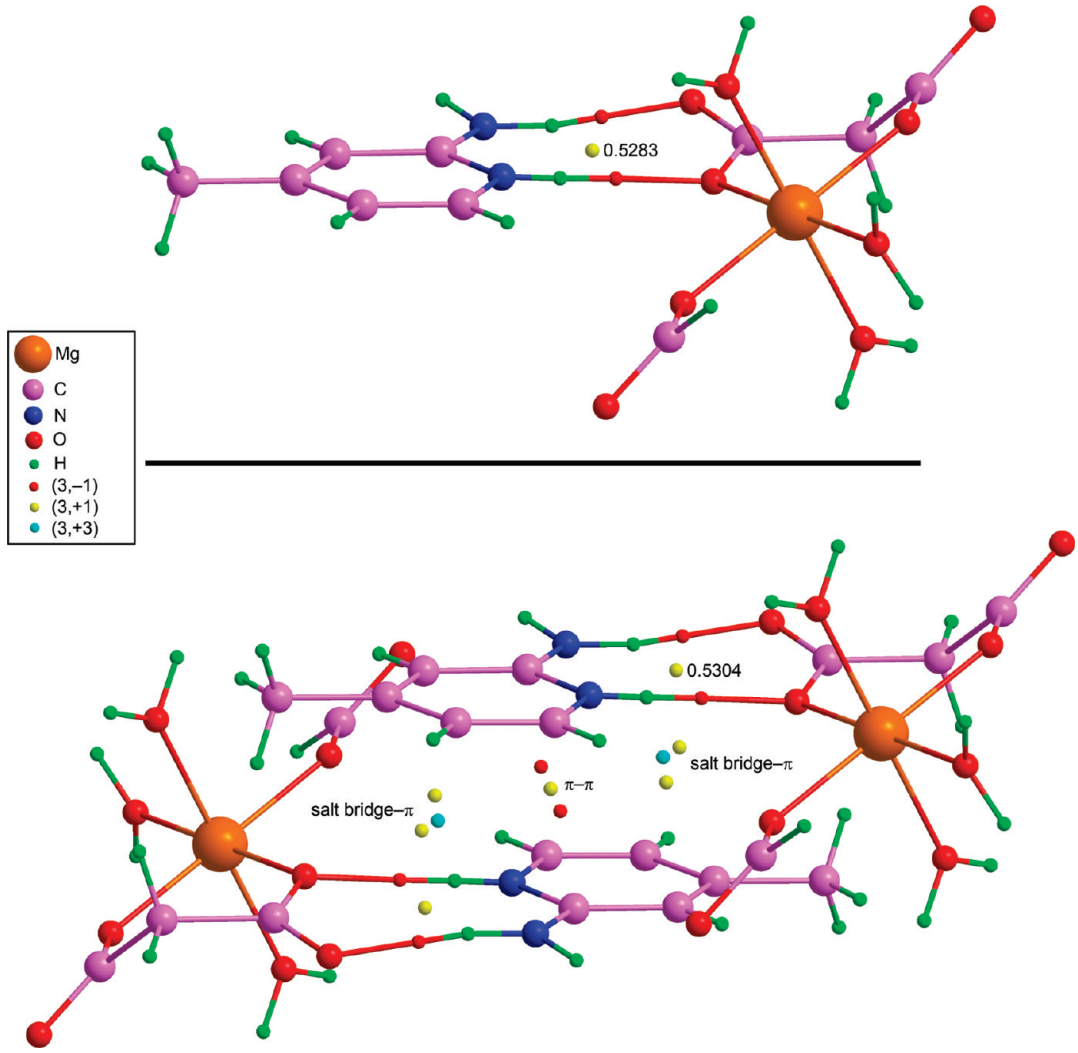

Figure 13. AIM analysis of two portions of the crystal structure of complex **2**. The numbers correspond to the value of the charge density ($10^2 \times \rho$) in atomic units, computed at the ring critical point that characterizes the salt bridge.

structure are shown in Figure 13. The first fragment is the salt-bridge-like interaction between the malonate ligand and the 2-amino-4-picolinium cation. It is characterized by two bonds and one ring CP. Some interesting issues arise from the inspection of the critical points obtained for the second fragment. This fragment is composed by two cations and two anions, and the stacking characteristics between the 2-amino-4-picoline rings have been studied. The $\pi\cdots\pi$ aromatic interaction is characterized by two bonds and one ring CP. Interestingly, some critical points appear between the salt-bridge and the picoline rings. Remarkably, a cage critical point, connecting the ring critical point that defines the salt bridge with the ring critical point of the aromatic ring, is present (not shown in Figure 13). This feature clearly indicates the occurrence of a double salt-bridge$\cdots\pi$ interaction in this system. The value of the charge density computed at the ring CP that characterized the salt-bridge is shown in Figure 13. Interestingly, the value is higher in the quaternary complex (bottom) than in the binary complex (top). This indicates that the salt-bridge is reinforced by the presence of the aromatic ring, in agreement with previous results.[82] The overall interaction energy of the neutral quaternary system is -6.34 kcal mol^{-1} at the RI-B97-D/TZVP level of theory.

Conclusion

In summary, the complexes herein described elegantly demonstrate that the primary structural motifs that constitute the backbone of the net supramolecular arrangement are dictated by hydrogen bonds (supramolecular synthons), whereas weaker and less well-defined interactions (lone pair$\cdots\pi$, anion$\cdots\pi$, and $\pi\cdots\pi$ contacts) are found to govern the final solid-state packing of the molecules, either in combination (such as the lone pair$\cdots\pi/\pi\cdots\pi/\pi\cdots$anion$\cdots\pi/\pi\cdots$lone association in **1**) or in an individual manner (like the lone pair$\cdots\pi$, $\pi\cdots\pi$ and salt-bridge $\cdots$ π contacts in **2**). The investigation herein reported also reflects that a complete prediction of the self-assembly of crystalline materials is obviously still not possible. Indeed, a mere change in counteranion can bring dramatic structural changes in the solid-state packing of molecules. Crystal engineering comprises in-depth understanding of weak intermolecular forces that govern crystal packing, thus potentially allowing a rational design of solids with tailored physical and chemical properties. The results described above are certainly of great importance in this regard. Intensive investigations are currently carried out in our laboratory to recognize various newer types of weak interactions, which can indeed be stabilizing and should not just be interpreted as short contacts. Recent developments are also shedding light in this direction,[83,84] and the present

study certainly helps to gain knowledge in this emerging area of supramolecular chemistry.

Acknowledgment. A.D. gratefully acknowledges University Grants Commission (New Delhi) for a research fellowship under the scheme "UGC Research Fellowship in Science for Meritorious Students 2007−2008". S.M. is grateful to UGC-CAS programme in the Department of Chemistry, Jadavpur University, for financial support of this work. C.E. thanks the MEC of Spain for a fellowship. We thank the MICINN of Spain (project CTQ2008-00841/BQU) for financial support. We thank the Centre de Supercomputació de Catalunya (CESCA) for computational facilities.

Supporting Information Available: Full crystallographic data in CIF format for **1** and **2** have been deposited with the Cambridge Crystallographic Data Center (CCDC Nos. 744082 and 744081, respectively, for **1** and **2**). Copies of these data can be obtained, free of charge, on application to CCDC, 12 Union Road, Cambridge, CB2 1EZ, U.K.; fax +44(0)-1223-336033; e-mail deposit@ccdc.cam.ac.uk. This material is available free of charge via the Internet at http://pubs.acs.org.

References and Notes

(1) Desiraju, G. R. *Crystal Engineering: The Design of Organic Solids*; Elsevier Science Publishers, B. V.: Amsterdam, The Netherlands, 1989.
(2) Biradha, K. *CrystEngComm* **2003**, *5*, 374–384.
(3) Zaworotko, M. J. *Chem. Commun.* **2001**, 1–9.
(4) Holman, K. T.; Pivovar, A. M.; Swift, J. A.; Ward, M. D. *Acc. Chem. Res.* **2001**, *34*, 107–118.
(5) Aakeröy, C. B.; Beatty, A. M.; Helfrich, B. A. *Angew. Chem., Int. Ed.* **2001**, *40*, 3240–3242.
(6) Aakeröy, C. B. *Acta Crystallogr.* **1997**, *B53*, 569–586.
(7) Desiraju, G. R. *Acc. Chem. Res.* **2002**, *35*, 565–573.
(8) Brammer, L. *Chem. Soc. Rev.* **2004**, *33*, 476–489.
(9) Braga, D.; Brammer, L.; Champness, N. R. *CrystEngComm* **2005**, *7*, 1–19.
(10) (a) Braga, D.; Desiraju, G. R.; Miller, J. S.; Orpen, A. G.; Price, S. L. *CrystEngComm* **2002**, *4*, 500–509. (b) Hong, B. H.; Bae, S. C.; Lee, C.-W.; Jeong, S.; Kim, K. S. *Science* **2001**, *294*, 348–351. (c) Singh, N. J.; Lee, H. M.; Hwang, I.-C.; Kim, K. S. *Supramol. Chem.* **2007**, *19*, 321–332.
(11) (a) Jana, A. D.; Manna, S. C.; Rosair, G. M.; Drew, M. G. B.; Mostafa, G.; Chaudhuri, N. R. *Cryst. Growth Des.* **2007**, *7*, 1365–1372, and references therein. (b) Singh, N. J.; Lee, H. M.; Suh, S. B.; Kim, K. S. *Pure Appl. Chem.* **2007**, *79*, 1057–1075. (c) Lee, J. Y.; Hong, B. H.; Kim, W. Y.; Min, S. K.; Kim, Y.; Jouravlev, M. V.; Bose, R.; Kim, K. S.; Hwang, I.-C.; Kaufman, L. J.; Wong, C. W.; Kim, P.; Kim, K. S. *Nature* **2009**, *460*, 498–501.
(12) Samai, S.; Biradha, K. *CrystEngComm* **2009**, *11*, 482–492.
(13) Thakur, T. S.; Desiraju, G. R. *Cryst. Growth Des.* **2008**, *8*, 4031–4044.
(14) Price, S. L. *Acc. Chem. Res.* **2009**, *42*, 117–126.
(15) Jeffrey, G. A. *An Introduction to Hydrogen Bonding*; Oxford University Press: Oxford, U.K., 1997.
(16) Desiraju, G. R.; Steiner, T. *The Weak Hydrogen Bond in Structural Chemistry and Biology*; Oxford University Press: Oxford, U.K., 1999.
(17) Desiraju, G. R. *Nature* **2001**, *412*, 397–400.
(18) (a) Beatty, A. M. *CrystEngComm* **2001**, *51*, 1–13. (b) Pak, C.; Lee, H. M.; Kim, J. C.; Kim, D.; Kim, K. S. *Struct. Chem.* **2005**, *16*, 187–202. (c) Lee, H. M.; Suh, S. B.; Lee, J. Y.; Tarakeshwar, P.; Kim, K. S. *J. Chem. Phys.* **2000**, *112*, 9759–9772. (d) Hong, B. H.; Lee, J. Y.; Lee, C.-W.; Kim, J. C.; Bae, S. C.; Kim, K. S. *J. Am. Chem. Soc.* **2001**, *123*, 10748–10749.
(19) Steiner, T. *Angew. Chem., Int. Ed.* **2002**, *41*, 48–76.
(20) (a) Hunter, C. A.; Sanders, J. K. M. *J. Am. Chem. Soc.* **1990**, *112*, 5525–5534. (b) Burley, S. K.; Petsko, G. A. *Science* **1985**, *229*, 23–28.
(21) (a) Kim, K. S.; Tarakeshwar, P.; Lee, J. Y. *Chem. Rev.* **2000**, *100*, 4145–4185. (b) Lee, E. C.; Kim, D.; Jurecka, P.; Tarakeshwar, P.; Hobza, P.; Kim, K. S. *J. Phys. Chem A* **2007**, *111*, 3446–3457. (c) Singh, N. J.; Min, S. K.; Kim, D. Y.; Kim, K. S. *J. Chem. Theor. Comput.* **2009**, *5*, 515–529.
(22) Janiak, C. *J. Chem. Soc., Dalton Trans.* **2000**, 3885–3896.
(23) Meyer, E. A.; Castellano, R. K.; Diederich, F. *Angew. Chem., Int. Ed.* **2003**, *42*, 1210–1250.
(24) (a) Ma, J. C.; Dougherty, D. A. *Chem. Rev.* **1997**, *97*, 1303–1324. (b) Kim, D.; Hu, S.; Tarakeshwar, P.; Kim, K. S.; Lisy, J. M. *J. Phys. Chem. A* **2003**, *107*, 1228–1238. (c) Kim, K. S.; Lee, J. Y.; Lee, S. J.; Ha, T.-K.; Kim, D. H. *J. Am. Chem. Soc.* **1994**, *116*, 7399–7400.
(25) (a) Nishio, M.; Hirota, M.; Umezawa, Y. *The C-H/π Interaction: Evidence, Nature and Consequences*; Wiley-VCH: New York, 1998. (b) Nishio, M. *CrystEngComm* **2004**, *6*, 130–158.
(26) (a) Burley, S. K.; Petsko, G. A. *Science* **1985**, *229*, 23–28. (b) Kim, K. S.; Tarakeshwar, P.; Lee, J. Y. *J. Am. Chem. Soc.* **2001**, *123*, 3323–3331.
(27) Mascal, M.; Armstrong, A.; Bartberger, M. D. *J. Am. Chem. Soc.* **2002**, *124*, 6274–6276.
(28) Alkorta, I.; Rozas, I.; Elguero, J. *J. Am. Chem. Soc.* **2002**, *124*, 8593–8598.
(29) Quiñonero, D.; Garau, C.; Rotger, C.; Frontera, A.; Ballester, P.; Costa, A.; Deyà, P. M. *Angew. Chem., Int. Ed.* **2002**, *41*, 3389–3392.
(30) (a) Gil-Ramirez, G.; Escudero-Adan, E. C.; Benet-Buchholz, J.; Ballester, P. *Angew. Chem., Int. Ed.* **2008**, *47*, 4114–4118. (b) Mooibroek, T. J.; Black, C. A.; Gamez, P.; Reedijk, J. *Cryst. Growth Des.* **2008**, *8*, 1082–1093.
(31) (a) Kim, D.; Tarakeshwar, P.; Kim, K. S. *J. Phys. Chem. A* **2004**, *108*, 1250–1258. (b) Kim, D.; Lee, E. C.; Kim, K. S.; Tarakeshwar, P. *J. Phys. Chem. A* **2007**, *111*, 7980–7986. (c) Kim, D. Y.; Singh, N. J.; Lee, J. W.; Kim, K. S. *J. Chem. Theor. Comput.* **2008**, *4*, 1162–1169. (d) Kim, D. Y.; Singh, N. J.; Kim, K. S. *J. Chem. Theor. Comput.* **2008**, *4*, 1401–1407.
(32) Gamez, P.; Mooibroek, T. J.; Teat, S. J.; Reedijk, J. *Acc. Chem. Res.* **2007**, *40*, 435–444.
(33) Schottel, B. L.; Chifotides, H. T.; Dunbar, K. R. *Chem. Soc. Rev.* **2008**, *37*, 68–83.
(34) Hay, B. P.; Bryantsev, V. S. *Chem. Commun.* **2008**, 2417–2428.
(35) Götz, R. J.; Robertazzi, A.; Mutikainen, I.; Turpeinen, U.; Gamez, P.; Reedijk, J. *Chem. Commun.* **2008**, *338*, 4–3386, and references cited therein.
(36) Egli, M.; Sarkhel, S. *Acc. Chem. Res.* **2007**, *40*, 197–205.
(37) Egli, M.; Gessner, R. V. *Proc. Natl. Acad. Sci. U.S.A.* **1995**, *92*, 180–184.
(38) Bancroft, D.; Williams, L. D.; Rich, A.; Egli, M. *Biochemistry* **1994**, *33*, 1073–1086.
(39) Sarkhel, S.; Rich, A.; Egli, M. *J. Am. Chem. Soc.* **2003**, *125*, 8998–8999.
(40) Calabrese, J. C.; Jordan, D. B.; Boodhoo, A.; Sariaslani, S.; Vannelli, T. *Biochemistry* **2004**, *43*, 11403–11416.
(41) Mooibroek, T. J.; Gamez, P.; Reedijk, J. *CrystEngComm* **2008**, *10*, 1501–1515.
(42) (a) de Hoog, P.; Robertazzi, A.; Mutikainen, I.; Turpeinen, U.; Gamez, P.; Reedijk, J. *Eur. J. Inorg. Chem.* **2009**, 2684–2690. (b) Kitson, P. J.; Song, Y. F.; Gamez, P.; de Hoog, P.; Long, D. L.; Parenty, A. D. C.; Reedijk, J.; Cronin, L. *Inorg. Chem.* **2008**, *47*, 1883–1885. (c) Lu, Z. L.; Gamez, P.; Mutikainen, I.; Turpeinen, U.; Reedijk, J. *Cryst. Growth Des.* **2007**, *7*, 1669–1671. (d) Mooibroek, T. J.; Teat, S. J.; Massera, C.; Reedijk, J. *Cryst. Growth Des.* **2006**, *6*, 1569–1574.
(43) Choudhury, S. R.; Gamez, P.; Robertazzi, A.; Chen, C.-Y.; Lee, H. M.; Mukhopadhyay, S. *Cryst. Growth Des.* **2008**, *8*, 3773–3784.
(44) Choudhury, S. R.; Dey, B.; Das, S.; Gamez, P.; Robertazzi, A.; Chen, C.-Y.; Lee, H. M.; Mukhopadhyay, S. *J. Phys. Chem. A* **2009**, *113*, 1623–1627.
(45) García-Raso, A.; Albertí, F. M.; Fiol, J. J.; Tasada, A.; Barceló-Oliver, M.; Molins, E.; Estarellas, C.; Frontera, A.; Quiñonero, D.; Deyà, P. M. *Cryst. Growth Des.* **2009**, *9*, 2362–2376.
(46) Garcia-Raso, A.; Albertí, F. M.; Fiol, J. J.; Tasada, A.; Oliver, M. B.; Molins, E.; Escudero, D.; Frontera, A.; Quiñonero, D.; Deyà, P. M. *Eur. J. Org. Chem.* **2007**, 5821–5825.
(47) Williams, J. M.; Ferraro, J. R.; Thorn, R. J.; Carlson, K. D.; Geier, U.; Wang, H. H.; Kini, A. M.; Whangbo, M.-H. *Organic Superconductors*; Prentice Hall: Englewood Cliffs, NJ, 1992.
(48) Dai, J.; Kuroda-Sowa, T.; Munakata, M.; Maekawa, M.; Suenaga, Y.; Ohno, Y. *J. Chem. Soc., Dalton Trans.* **1997**, 2363–2368.
(49) Iwaoka, M.; Takemoto, S.; Okada, M.; Tomoda, S. *Bull. Chem. Soc. Jpn.* **2002**, *75*, 1611–1625.
(50) Werz, D. B.; Gleiter, R.; Rominger, F. *J. Am. Chem. Soc.* **2002**, *124*, 10638–10639.
(51) Gleiter, R.; Werz, D. B.; Rausch, B. J. *Chem.—Eur. J.* **2003**, *9*, 2676–2683.
(52) Kobayashi, K.; Masu, H.; Shuto, A.; Yamaguchi, K. *Chem. Mater.* **2005**, *17*, 6666–6673.
(53) Manna, S. C.; Jana, A. D.; Drew, M. G. B.; Mostafa, G.; Chaudhuri, N. R. *Polyhedron* **2008**, *27*, 1280–1286.
(54) Ghosh, R.; Jana, A. D.; Pal, S.; Mostafa, G.; Fun, H.-K.; Ghosh, B. K. *CrystEngComm* **2007**, *9*, 353–357, and references therein.
(55) Jana, A. D.; Ghosh, A. K.; Ghoshal, D.; Mostafa, G.; Chaudhuri, N. R. *CrystEngComm* **2007**, *9*, 304–312, and references therein.
(56) Wozniak, K.; He, H.; Klinowski, J.; Jones, W.; Grech, E. *J. Phys. Chem.* **1994**, *98*, 13755–13765.

(57) Ni, B.; Lee, K. H.; Sinnott, S. B. *J. Phys.: Condens. Matter* **2004**, *16*, 7261–7275.
(58) Breza, M.; Biskupic, S.; Manova, A. *Polyhedron* **2003**, *22*, 2863–2867.
(59) Jenkins, S.; Morrison, I. *Chem. Phys. Lett.* **2000**, *317*, 97–102.
(60) Lemos, M. C.; Luque, J. J.; Jimenez-Morales, F. *J. Chem. Phys.* **1998**, *109*, 8069–8075.
(61) Blake, N. P.; Weakliem, P. C.; Metiu, H. *J. Phys. Chem. B* **1998**, *102*, 67–74.
(62) Igarashi, K.; Tajiri, K.; Tanemura, S.; Nanbu, R.; Fukunaga, T. *Z. Phys. D: At., Mol. Clusters* **1997**, *40*, 562–567.
(63) Dang, L. X. *J. Chem. Phys.* **1992**, *97*, 2659–2660.
(64) Raghavaiah, P.; Supriya, S.; Das, S. K. *Chem. Commun.* **2006**, 2762–2764.
(65) Bleiholder, C.; Werz, D. B.; Köppel, H.; Gleiter, R. *J. Am. Chem. Soc.* **2006**, *128*, 2666–2674.
(66) Sanz, P.; Yáñez, M.; Mó, O. *Chem.—Eur. J.* **2003**, *9*, 4548–4555.
(67) Bleiholder, C.; Gleiter, R.; Werz, D. B.; Koppel, H. *Inorg. Chem.* **2007**, *46*, 2249–2260.
(68) Choudhury, S. R.; Dey, B.; Das, S.; Robertazzi, A.; Jana, A. D.; Chen, C.-Y.; Lee, H. M.; Gamez, P.; Mukhopadhyay, S. *Dalton Trans.* **2009**, 7617–7624.
(69) (a) Bader, R. F. W. *Chem. Rev.* **1991**, *91*, 893–928. (b) Bader, R. F. W. *Atoms in Molecules. A Quantum Theory*; Clarendon: Oxford, U.K., 1990.
(70) Sheldrick, G. M. *SHELXL97: Program for the Refinement of Crystal Structures*; University of Göttingen: Göttingen, Germany, 1997.
(71) Ahlrichs, R.; Bär, M.; Häser, M.; Horn, H.; Kölmel, C. *Chem. Phys. Lett.* **1989**, *162*, 165–169.
(72) Quiñonero, D.; Garau, C.; Frontera, A.; Ballester, P.; Costa, A.; Deyà, P. M. *J. Phys. Chem. A* **2006**, *110*, 5144–5157.
(73) König, F. B.; Schönbohm, J.; Bayles, D. *J. Comput. Chem.* **2001**, *22*, 545–559.
(74) Rybarczyk-Pirek, A. J.; Dubis, A. T.; Grabowski, S. J.; Nawrot-Modranka, J. *Chem. Phys.* **2006**, *320*, 247–258.
(75) Howard, S. T.; Lamarche, O. *J. Phys. Org. Chem.* **2003**, *16*, 133–141.
(76) Drevensek, P.; Kosmrlj, J.; Giester, G.; Skauge, T.; Sletten, E.; Sepcic, K.; Turel, I. *J. Inorg. Biochem.* **2006**, *100*, 1755–1763.
(77) Gentile, P. S.; White, J. G.; Dinstein, M. P.; Bray, D. D. *Inorg. Chim. Acta* **1977**, *21*, 141–144.
(78) Morosin, B. *Acta Crystallogr.* **1967**, *22*, 315–320.
(79) Schmidt, M.; Schier, A.; Schmidbaur, H. *Z. Naturforsch., B* **1998**, *53*, 1098–1102.
(80) Pasán, J.; Sanchiz, J.; Lloret, F.; Julve, M.; Ruiz-Pérez, C. *CrystEngComm* **2007**, *9*, 478–487, and references cited therein.
(81) Bondi, A. *J. Phys. Chem.* **1964**, *68*, 441–451.
(82) Thompson, S. E.; Smithrud, D. B. *J. Am. Chem. Soc.* **2002**, *124*, 442–449.
(83) Drew, M. G. B.; De, S.; Nag, S.; Datta, D. *Inorg. Chim. Acta* **2009**, *362*, 610–613.
(84) Tian, Z.-F.; Duan, H.-B.; Zhou, H.; Ren, X.-M.; Zhang, H.; Meng, Q.-J. *Inorg. Chem. Commun.* **2009**, *12*, 148–150.

JP911884X